Adsorption (2011) 17: 527–538
DOI 10.1007/s10450-010-9315-1

Preparation, characterization and catalytic applications of ZrO_2 supported on low cost SBA-15

Álvaro Reyes-Carmona · Ramón Moreno-Tost · Josefa Mérida-Robles · José Santamaría-González · Pedro J. Maireles-Torres · Antonio Jiménez-López · Elisa Moretti · Maurizio Lenarda · Enrique Rodríguez-Castellón

Received: 26 October 2010 / Accepted: 21 December 2010 / Published online: 6 January 2011

Abstract This work presents some applications of ZrO_2 supported over SBA-15 silica as promoter of sulfated zirconia and as support from CuO/CeO_2 catalytic system for preferential oxidation of CO to CO_2 in hydrogen rich streams, used as feed for proton exchange membrane fuel cells (PEMFC). Different amounts of ZrO_2, from 10 to 30 wt.% were incorporated. These prepared materials were characterized by powder XRD, adsorption-desorption of N_2 at 77 K, transmission and scanning electron microscopy (TEM and SEM) and X-rays photoelectron spectroscopy (XPS). The acidity was studied by thermo-programmed desorption of ammonia (NH_3-TPD). These materials were tested, after treatment with H_2SO_4, by 2-propanol dehydration and 1-butene isomerization catalytic tests. The samples were found quite good catalyst with strong acid sites, the sample with 20 wt.% of ZrO_2 being the better performing sample. Finally this material was successfully used as support for a CuO/CeO_2 system, with 6 wt.% of Cu and 20 wt.% of Ce. The resulting catalyst was tested in the preferential oxidation of CO (CO-PROX) attaining conversions close to 100% and high selectivity to CO_2.

Keywords SBA-15 · ZrO_2 · Sulfated zirconia · CuO/CeO_2 · PROX

Á. Reyes-Carmona · R. Moreno-Tost · J. Mérida-Robles · J. Santamaría-González · P.J. Maireles-Torres · A. Jiménez-López · E. Rodríguez-Castellón (✉)
Departamento de Química Inorgánica, Cristalografía y Mineralogía (Unidad Asociada al ICP-CSIC), Facultad de Ciencias, Universidad de Málaga, Campus de Teatinos, 29071 Málaga, Spain
e-mail: castellon@uma.es

E. Moretti · M. Lenarda
Dipartimento di Chimica, Università Ca' Foscari di Venezia, Via Torino 155/B, 30172 Venezia, Italy

1 Introduction

Mesoporous materials have been widely studied since the publication of the work of Beck group (Beck et al. 1992), reporting the first description of ordered mesoporous MCM-41 type silicas. Some years after this work, scientists at Santa Barbara University reported the preparation of the SBA-15 type materials, which showed better hydrothermal properties and wide pore diameters than MCM-41 (Zhao et al. 1998). Since these two works, a lot of papers were published on materials with these morphologies (Berggen et al. 2005). One of the main applications of this type of porous materials is their use as precursors or supports of active phase catalysts.

On the other hand, it is well known that sulfated zirconia is be well suited to catalyze various reactions of industrial importance, which involve acid active sites, like the isomerization, dehydration or alkylation of hydrocarbons and alcohols (Yadav and Nair 1999).

Sulfated zirconia was found to better perform when supported on well known oxides like γ-Al_2O_3 (Sohn and Seo 2003) and more recently, over synthesized mesoporous materials (Akkari et al. 2007; Fuxiang et al. 2007).

The preferential oxidation of CO (CO-PROX) is a catalytic process with high impact in fuel cell technology. The most efficient fuel cell system for mobile systems is the polymer electrolyte membrane fuel cell (PEMFC). This fuel cell requires a hydrogen stream feed virtually without CO, because less than 100 ppm can poison the platinum electrode. To avoid this phenomena, several processes were studied (Park et al. 2009), finding CO-PROX as the most promising for a further implementation in mobile systems.

Several catalytic systems were studied; supported platinum family metals, gold supported on ceria or iron oxide and supported metal oxides, like CuO over ceria. This last

fact was carefully studied (Liu et al. 1995; Martínez-Arias et al. 2000) and is considered one of the best options as catalytic system for PROX reaction at the PEM fuel cells operative conditions.

The CuO/CeO_2 system has shown a performance improvement in presence of elements able to create acid centers, like Al (Moretti et al. 2007, 2008) or Zr (Ratnasamy et al. 2004; Moretti et al. 2009). Some authors (Liu et al. 2004; Ratnasamy et al. 2004; Manzoli et al. 2005) have studied the influence of Zr on the catalytic performance of CuO/CeO_2 system for the CO-PROX, finding an increase of the conversion of CO and of the selectivity to CO_2. We tested the system supported over SBA-15 with Zr incorporated in the inner structure and as catalyst for CO-PROX reaction with conversions close to 100%. Following our studies on CuO/CeO_2 supported on SBA-15 type oxides (Reyes-Carmona et al. 2010) as catalyst for the CO-PROX, in this work, we describe the preparation of supported zirconia over a low-cost SBA-15 and its treatment with H_2SO_4 to obtain sulfated zirconia and zirconium sulfate. These materials, after characterization, were tested with the 2-propanol conversion and 1-butene isomerization tests and as support for the CuO/CeO_2 system in the catalytic PROX of CO in a rich hydrogen stream.

2 Experimental

2.1 Material synthesis

2.1.1 Mesoporous silica SBA-15

SBA-15 mesoporous silica was synthesized using a low-cost method as described elsewhere (Gómez-Cazalilla et al. 2007) and the preparation is summarized as follows: 5 g of Pluronic ($EO_{20}PO_{70}EO_{20}$ from Aldrich) were added to 200 mL of 0.4M H_2SO_4 solution. After stirring for a few hours, a clear solution was obtained. Then, 0.2 g of NaOH and 13.3 mL of sodium silicate solution ($Na_2Si_3O_7$ with 27% SiO_2 and 14% NaOH from Aldrich) were added at room temperature with stirring. The resulting gel mixture was stirred for 5 days at room temperature. The solid product was recovered by filtration, washed several times with water and dried overnight at 333 K. Finally, the material was calcined in static atmosphere at 823 K for 6 h using a heating rate of 10 K min^{-1}.

2.1.2 Supported sulfated zirconia materials

Zirconium oxide was supported over the SBA-15 silica by the incipient wetness impregnation method, adding a solution of zirconium(IV) acetate (Aldrich), in order to obtain materials with 10, 20 and 30 wt.% of ZrO_2. All the materials were dried overnight at 333 K and calcined using a tubular quartz oven with a synthetic air flow of 100 mL min^{-1} to 653 K for 4 h with a heating ramp of 1 K min^{-1}. These materials were labeled as SZX, where X is the wt.% of ZrO_2 supported.

These materials were treated with 4M H_2SO_4 solution via incipient wetness impregnation method (3 ml g^{-1}) and were dried overnight at 333 K and calcined to 823 K for 3 h with a heating ramp of 1 K min^{-1}. These materials were labeled as SZXS, where X is the wt.% of ZrO_2 supported.

2.1.3 CO-PROX catalyst

The active phase was incorporated over SZ20 sample by incipient wetness using an aqueous solution of copper(II) and cerium(III) acetates (both from Aldrich). The loading of copper was 6 wt.% and cerium was 20 wt.%. These amounts were found as optimal in previous works (Moretti et al. 2009; Reyes-Carmona et al. 2010). Due to the limited solubility of the salts, the impregnation was carried out in several steps until the total incorporation of the salts. The material was dried overnight at 333 K and calcined at 823 K for 4 h in static atmosphere with a heating ramp of 1 K min^{-1}. For comparison, a material with the same amount of Cu and Ce was synthesized, using pristine SBA-15 as support. Samples were labeled SZ20Ce20Cu6 and SBACe20Cu6, respectively.

2.2 Characterization methods

2.2.1 XRD

X-ray diffraction (XRD) patterns were obtained with a *Philips X'pert PRO* apparatus using Cu Kα_1 radiation ($\lambda = 0.1540$ nm) with a Ge (111) monochromator working at 45 kV and 35 mA. All the measurements were made with a step size of 0.0167° in 30 minutes.

2.2.2 Adsorption-desorption of nitrogen

N_2 adsorption-desorption measurements were performed at liquid nitrogen temperature (77 K) with an *ASAP 2020* apparatus from *Micromeritics*. Before each measurement, samples were out gassed 12 h at 473 K and 1×10^{-2} Pa. The specific surface (S_{BET}) was calculated using the BET equation, and the specific pore volume (v_p) was calculated at $P/P_0 = 0.98$. The pore size distribution was calculated following BJH method, taking the data of the desorption branch and assuming a cylindrical pore model.

2.2.3 TEM

Transmission electron micrographs were obtained with a *Philips CM200* microscope working at 10 kV. The measurements of X-ray dispersive energy were registered using an

EDAX CM200ST probe based in a detector SiLi. The samples were dispersed in 2-propanol and dropped over a Cu grid. Ni grids were used when copper was present in the samples in order to avoid interferences using EDX probe.

2.2.4 SEM

Scanning electron micrographs were obtained by using a JEOL SM 840 microscope. Samples were placed on an aluminum drum and metalized with a gold film using a JEOL Ion Sputter JFC 1100.

2.2.5 Elemental analysis

The elemental analysis (C, N, H, S elements) was performed on a LECO CHNS 932 analyzer.

2.2.6 NH_3-TPD

NH_3-TPD was used to determine the total acidity of the samples. Around 80 mg of sample was placed in the bulb of a quartz U tube. Before the adsorption of ammonia at 373 K, samples were heated to 823 K in a He flow. The ammonia desorbed between 373 and 823 K (heating rate of 10 $K\,min^{-1}$) was detected using an on-line gas chromatograph (Shimadzu GC-14A) provided with a TC detector. The response of the detector was calibrated using $[Ni(NH_3)_6]Cl_2$ as NH_3 source.

2.2.7 XPS

X-ray Photoelectron Spectroscopy (XPS) studies were realized by a *Physical Electronic PHI 5700* spectrometer using non monochromatic Mg K radiation (300 W, 15 kV, 1253.6 eV) for the analysis of the core level signals of C 1*s*, O 1*s*, Si 2*p*, S 2*p*, Cu 2*p*, Zr 3*d* and Ce 3*d* with a hemispherical multichannel detector. The spectra of powdered samples were registered with a constant pass energy values at 29.35 eV, using a 720 μm diameter circular analysis area. The X-ray photoelectron spectra obtained were analyzed with *PHI ACESS ESCA V6.0F* software and processed using *Multipak 8.2B* package. The binding energy values were referenced to C 1*s* signal (284.8 eV). Shirley type background and Gauss-Lorentz curves were used to determinate the binding energy. Short acquisition times (<10 min) were used in order to avoid photoreduction of copper and cerium species (Poulston et al. 1996).

2.3 Catalytic tests

2.3.1 Isopropanol test

The catalytic decomposition of isopropanol was used as a test reaction for the study of the effective acidity. A fixed bed tubular glass reactor working at atmospheric pressure was used for a solid charge of 25 mg without dilution (0.2–0.3 mm particle size). Samples were pretreated at 473 K in helium flow for 1 h (60 $mL\,min^{-1}$). Isopropanol was fed into the reactor by flowing through a saturator condenser at 303 K, which gave a constant isopropanol flow of 7.5 vol%, using a contact time $W/F = 0.41$ g_{cat} min $mmol^{-1}$, where F is the molar flow and W the weight of catalyst bed used. Tests were performed between 423 and 473 K. The reaction products were analyzed by an on-line gas chromatograph (Shimadzu GC-14A) provided with an FID and a fused silica capillary column SPB1. Propylene and diisopropylether (DIPE) were analyzed as unique products in our tests.

2.3.2 1-butene isomerization test

The catalytic isomerization of 1-butene was performed in a tubular glass flow microreactor. Samples (133 mg) were pretreated for 2 h in a He flow at 673 K (30 $mL\,min^{-1}$), and the experiments were carried out at this temperature. Experiments were performed at $W/F = 0.60$ $g_{cat}\,h\,mol^{-1}$ and the time on stream was 120 min. The reactant 1-butene and the reaction products were analyzed on-line in a gas chromatograph (Shimadzu GC-14B) equipped with a wide-bore $KCl/AlCl_3$ column. For this reaction, the distribution of butenes was close to the equilibrium point.

2.3.3 CO-PROX reaction test

Preferential oxidation of CO catalytic test was carried out in a tubular fixed bed reactor operating at atmospheric pressure. The catalysts were loaded in order to obtain a contact time $W/F = 0.18$ $g_{cat}\,s\,cm^{-3}$ or equivalently, gas hourly space velocity (GHSV) = 22000 h^{-1}. Previously, catalysts were activated at 673 K in air flow for 1 hour. The feed was a mixture of 1.25% CO, 1.25% O_2 and 50% H_2 balanced with He (% vol.). The piping was heated at 393 K in order to avoid water condensation after the reactor outlet. A HP6890 gas chromatograph equipped with a CP Carboplot P7 packed column and a TC detector was used to analyze the composition of the reactor outlet.

The temperature was varied in the 313–463 K range, and measurements were carried out after steady state reaching. Methanation and reverse water gas shift reaction were found to be unattainable in the experimental conditions. The activity of catalysts was measured by the CO conversion (Eq. 1):

$$x_{CO} = \frac{n_{CO}^{in} - n_{CO}^{out}}{n_{CO}^{in}} \times 100 \quad (1)$$

The selectivity towards CO_2 was estimated from the oxygen mass balance as follow (Eq. 2):

$$Sel_{CO_2} = \frac{n_{CO}^{in} - n_{CO}^{out}}{2(n_{O_2}^{in} - n_{O_2}^{out})} \times 100 \quad (2)$$

The excess oxygen factor (λ) is defined as (Eq. 3):

$$\lambda = 2 \times \frac{n_{O_2}^{in}}{n_{CO}^{in}} \quad (3)$$

3 Results and discussion

3.1 Characterization

3.1.1 X-ray diffraction

The SZX materials were analyzed after calcination at 653 K and the corresponding diffractograms are shown in Fig. 1. The most intense reflection line at 1.05° is assigned to the (100) diffraction plane of SBA-15, evidencing the hexagonal pore structure of these materials. The main reflections of tetragonal zirconium oxide (ICSD#01-079-1769) at 30.22, 50.22 and 60.20° are also observed, with the peaks intensity increasing with the increasing of the amount of supported zirconia. The average crystallite sizes were calculated by the Scherrer equation taking the values of the most intense (111) peak at 30.22°, obtaining sizes between 25–35 nm.

After impregnation with H_2SO_4 and calcination at 823 K, most of the zirconia was transformed into zirconium sulfate (ICSD#01-072-0608), as shown in Fig. 2. The main diffraction peaks in the samples with high load of ZrO_2. However, a small amount of zirconia was still detected, meaning not only that the reaction with sulfuric acid was not complete but also that the calcinations treatment did not lead to the transformation of tetragonal zirconia into the monoclinic phase (ICSD#01-078-1807) (Y.-W. Suh et al. 2003), that is known to occur at 773 K.

In Fig. 2 the diffraction patterns of CuO/CeO_2 supported materials before and after CO-PROX are also shown. Cerianite (ICSD#01-081-0792), assigned to CeO_2, and tenorite (ICSD#01-089-2529), assigned to CuO, phases were detected in the fresh materials. After reaction, a peak at $2\theta = 43.5°$, assigned to metallic Cu, appears in both samples. It is probably caused by the reduction of the CuO bulk particles. Diffraction peaks of tetragonal ZrO_2 (ICSD#01-079-1769) are still present in the XRD profile of sample SZ20Ce20Cu6. We discard the formation of solid solutions between ZrO_2 and CeO_2 phases (Reyes-Carmona et al. 2010).

3.1.2 Adsorption-desorption of N_2 at 77 K

The nitrogen adsorption-desorption isotherms of SZXS materials are shown in Fig. 3. The overall shapes of the isotherms and pore size distributions are similar; with a decrease in the adsorbed volume with an increase of the ZrO_2 load. These isotherms are of type IV according to the IUPAC classification and with H1 type hysteresis behavior, characteristic of mesoporous materials with well-defined cylindrical pores. The textural data obtained after application of BET and BJH methods are summarized in Table 1. All the materials show high specific surface areas, from 488 m^2g^{-1} for pristine SBA-15 to 339 m^2g^{-1} for SZ30S material and narrow pore size distributions with values around 3.1–3.8 nm. Data of CO-PROX catalytic materials are also shown in Fig. 4 and summarized in Table 1.

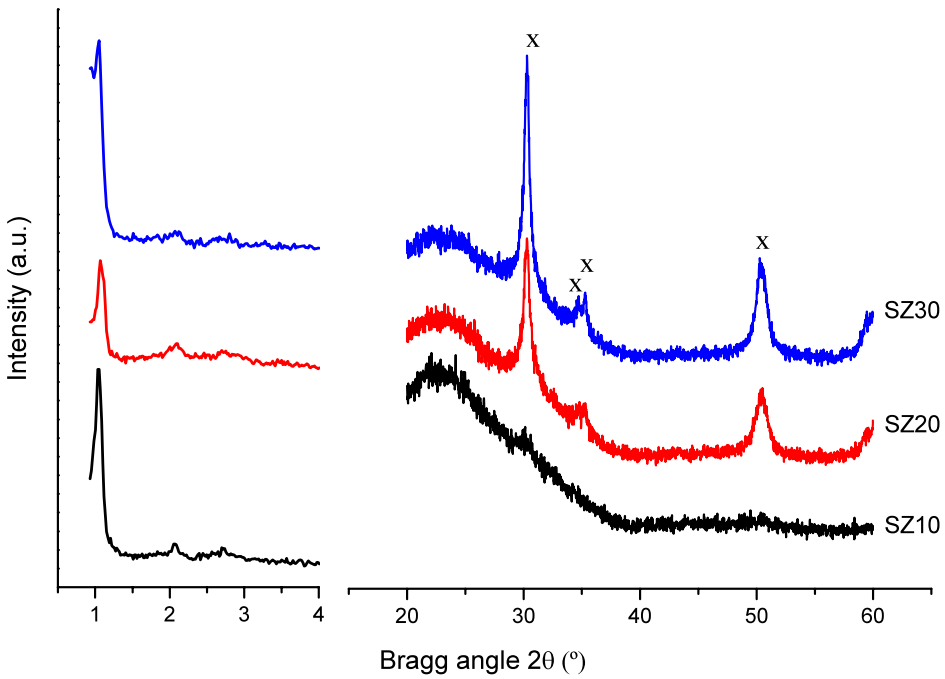

Fig. 1 X-ray diffraction patterns of SZX materials after calcination at 653 K. Peaks marked with x are assigned to tetragonal ZrO_2

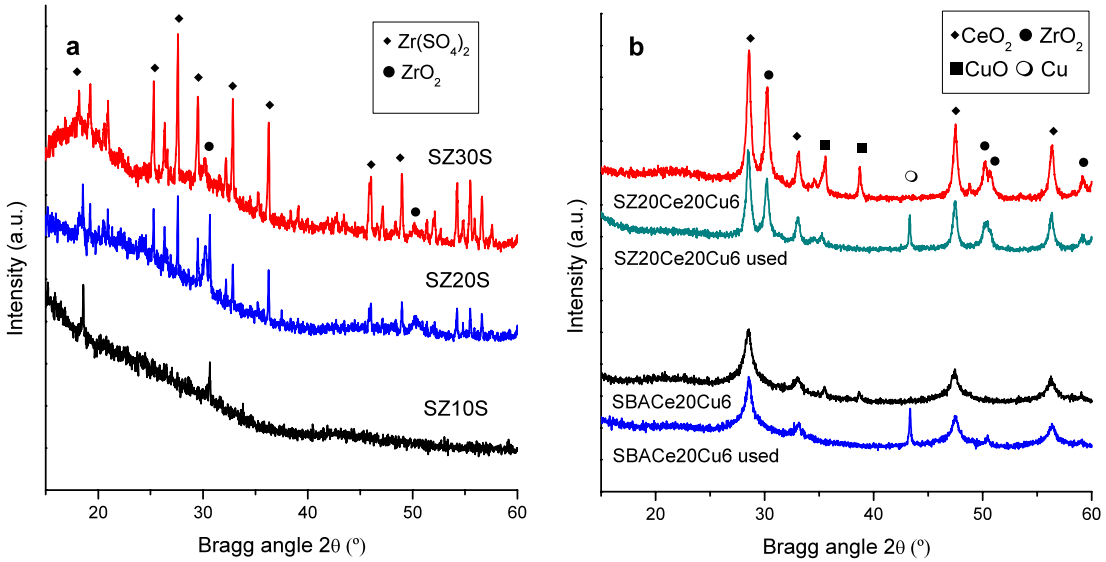

Fig. 2 **a** X-ray diffraction patterns of SZX materials after calcination at 823 K. **b** X-ray diffraction patters of PROX test catalysts fresh and used

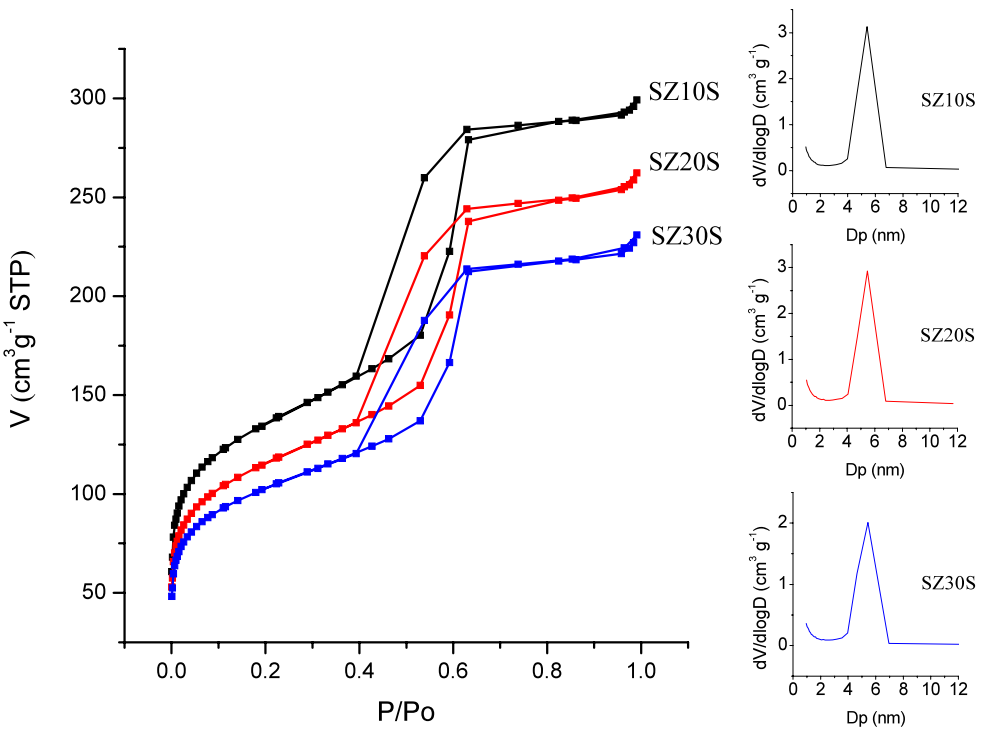

Fig. 3 Adsorption-desorption isotherms of N_2 at 77 K and pore distribution profile from SZXS samples

The incorporation of Ce and Cu oxides changes the shape of the isotherms to a H2 type, typical of partially blocked pore materials, more pronounced in the case of SBACe20Cu6 sample.

3.1.3 Microscopy and EDX data

In Fig. 5 a TEM micrography of SZ20S is shown. It is possible to observe the regular nanometric hexagonal pore structure of the SBA-15 support and the dark areas are assigned to a high concentration of Zr. Isolated particles of sulfated zirconia were not detected. X-ray dispersive energies spectra were recorded and one of them is shown in the inset of Fig. 5. Peaks associated to all the present elements were detected, Cu and Fe signals appearing to be due to the grid and chamber. Similar EDX spectra were found for all samples. In Fig. 6 the micrograph of the material labeled SZ20Ce20Cu6 is shown. Dark particles associated to CuO

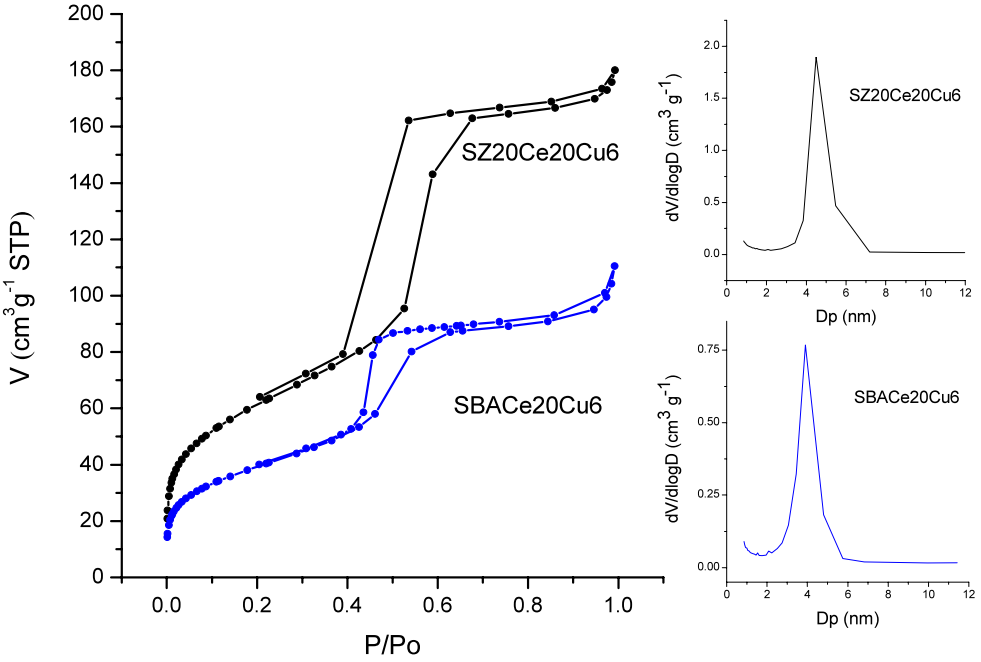

Fig. 4 Adsorption-desorption isotherms of N_2 at 77 K and pore distribution profile from PROX catalysts SZ20Ce20Cu6 and SBACe20Cu6

Table 1 Textural parameters of SZX materials

Sample	% ZrO_2 (wt%)	S_{BET} (m^2/g)	V_P (cm^3/g)	d_p BJH (nm)
SBA-15	0	488	0.48	3.0
SZ10S	10	453	0.45	3.1
SZ20S	20	383	0.40	3.2
SZ30S	30	339	0.35	3.1
SZ20	20	330	0.36	3.8
SZ20Ce20Cu6	20	215	0.27	3.6
SBACe20Cu6	0	139	0.35	3.8

clusters, in the nanometric range, can be shown while the mesoporous hexagonal habit of the support is maintained.

The microscale morphology of the materials is shown in the SEM micrograph presented in Fig. 7, where it shows the typical rod-shape of SBA-15 materials.

3.1.4 Elemental analysis

The content of S, as evidence of the sulfatation grade of SZXS materials, can be obtained by elemental analysis. Table 2 shows weight percentages of elements in the samples. Not a high amount of C was detected; this is an evidence of the total decomposition of the zirconium(IV) acetate used as precursor and of the surfactant used. An increase in the S amount was observed with the increasing amount the incorporated ZrO_2, reaching S percentages up to 6%.

3.1.5 Temperature-programmed desorption of NH_3

The amount and the strength of acid sites of supported sulfated zirconia materials, labeled as SZXS was studied by NH_3-TPD. Ammonia is an adequate probe molecule due to its small size and basicity, which allows the interaction which the majority of the acid sites. Thus, the amount of ammonia desorbed at some characteristic temperatures is taken as a measurement of the number of acid centers, while the temperature range in which the ammonia is desorbed is an indicator of the strength of the acid sites. Integration of these curves provides the histograms shown in Fig. 8. An increase of the total acidity with the added amount of ZrO_2 was observed, reaching values between 600 and 1345 μmol NH_3 g^{-1}. In these materials, most of ammonia is desorbed in the 473–573 K intervals, assigned to medium-strength Brönsted acid sites (Corma et al. 1994).

3.1.6 X-ray photoelectronic spectroscopy

Valuable information about chemical state and surface composition of the samples can be obtained by XPS. The materials were studied before and after treatment with sulfuric acid in order to get an insight in the modification of the chemical state of O and Zr, studying the O 1*s* and Zr 3*d* regions (Gracia et al. 2009). Binding energies of SZX materials are shown in Table 3. The Si 2*p* core level signal shows an intense peak centered at 103.7 eV, assigned to SBA-15 silica in tetrahedral sites. In all cases, the Zr 3*d* regions show a doublet, assigned to Zr(IV) with the contribution Zr $3d_{5/2}$ centered at 182.7 eV. However, the O 1*s* core level spectra show

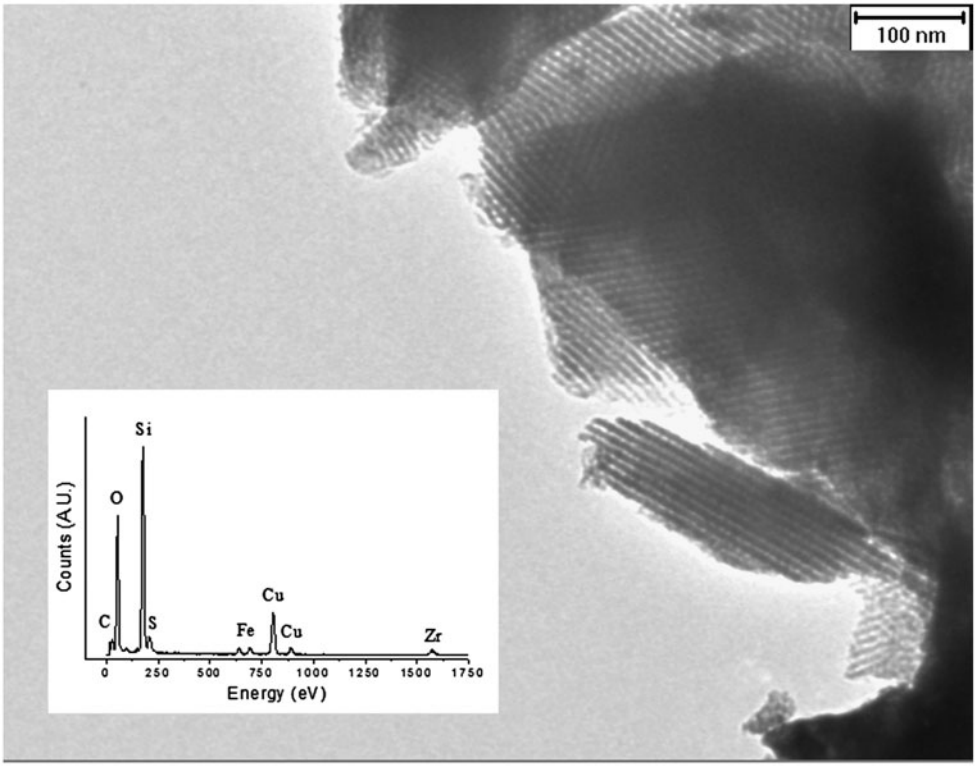

Fig. 5 Transmission electron micrograph and EDX spectrum of SZ20S sample

Table 2 Elemental analysis of SZXS materials

Sample	% C	% H	% N	% S
SBA-15	0.004	0.723	–	–
SZ10S	0.155	2.824	0.064	3.742
SZ20S	0.205	2.522	0.096	4.996
SZ30S	0.219	2.606	0.075	6.184

a marked asymmetry, which was decomposed in two contributions, one at 533.0 eV associated with silica oxygen and another one at 530.6 eV, typical of metallic oxides, in our case, ZrO_2. This evidence is supported with an increase of this last contribution with the increase of the amount of ZrO_2 added, as showed in Table 3. The observed Si/Zr atomic ratios are clearly indicating that ZrO_2 is incorporated to the porous structure.

After H_2SO_4 treatment, the samples were analyzed and the results are summarized in Table 4. In all cases, the Si $2p$ photoemission remains unaltered at 103.4 eV after treatment. A typical doublet is seen now in the S $2p$ region, assigned to S(VI) atoms from sulfate species, with a value of S $2p_{3/2} = 168.8$ eV. The Zr $3d_{5/2}$ peak is shifted to an average value of 183.3 eV due to the sulfatation. Finally, a shift in the O $1s$ signal to a lower binding energy (532.0 eV) was observed, probably due to the presence of sulfate species over the surface of the materials.

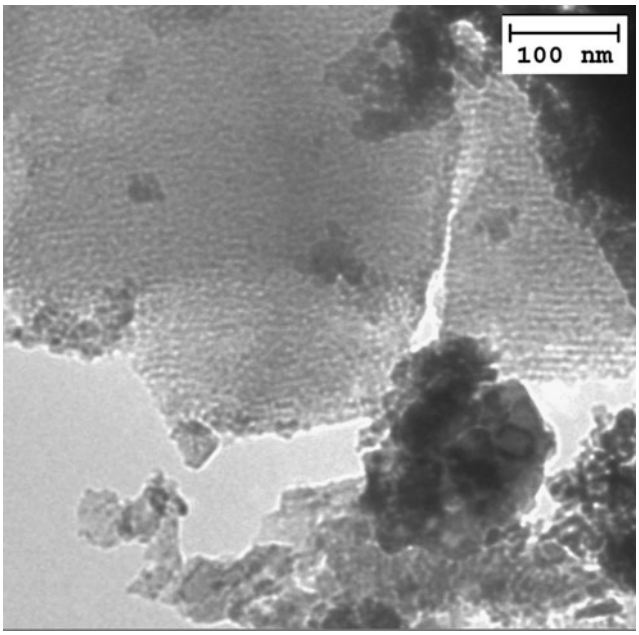

Fig. 6 Transmission electron micrograph of the fresh SZ20Ce20Cu6 material

Some interesting information can be obtained from the study of Cu $2p$ and Ce $3d$ regions, using the methodology of our recent works (Moretti et al. 2009; Reyes-Carmona et al. 2010). Data of binding energies and redox properties are collected in Table 4. Ce^{3+} percentage was calculated us-

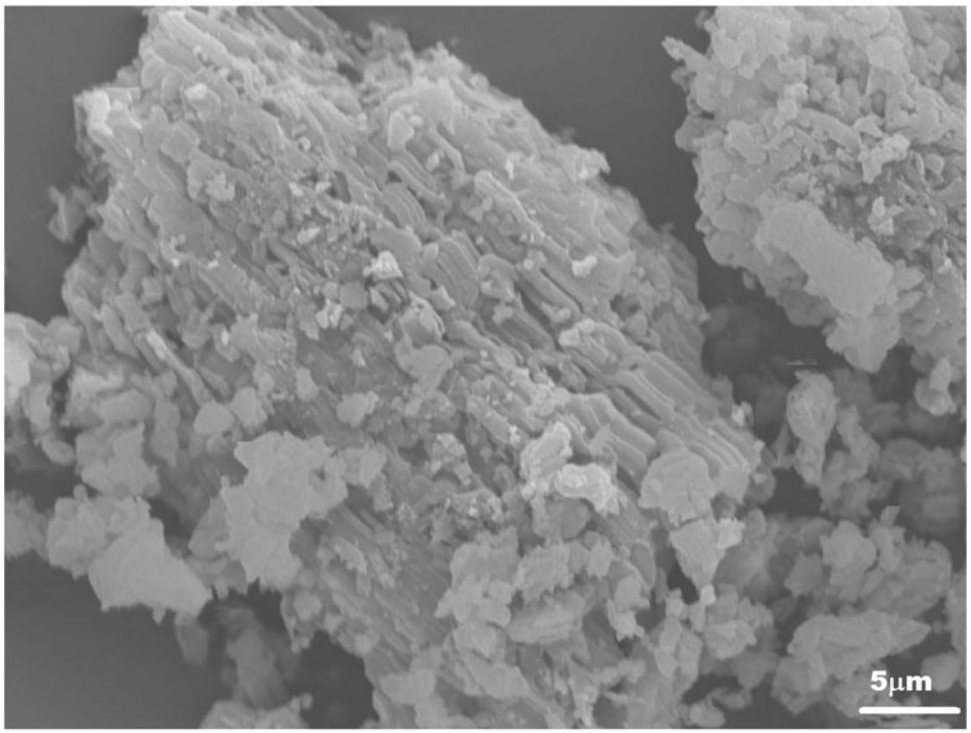

Fig. 7 Scanning electron micrograph of SZ20S sample

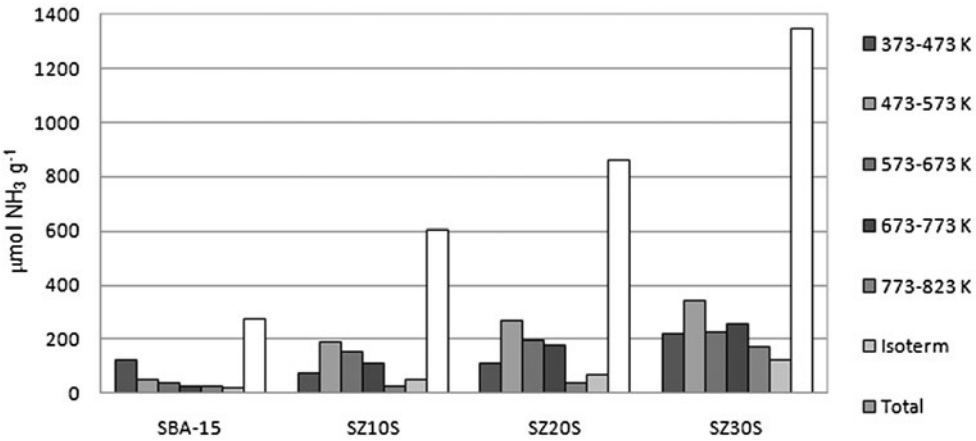

Fig. 8 Acidity distribution histograms of SZXS samples determined by NH_3-TPD

Table 3 XPS data from SZX materials

Sample	Si 2*p*	O 1*s*	Zr $3d_{5/2}$	Si/Zr atomic ratio (theorical)	Si/Zr atomic ratio (superficial)
SBA-15	103.8	533.1	–	–	–
SZ10	103.7	530.5 (25%)	182.6	18.5	3.4
		532.9 (75%)			
SZ20	103.7	530.7 (26%)	182.8	8.2	3.5
		533.0 (74%)			
SZ30	103.7	530.7 (32%)	182.8	4.8	2.3
		533.0 (68%)			

ing the ratio between the areas of Ce 3*d* core level peaks. O 1*s* region can be composed by two contributions, one at 529.8 eV, assigned to CeO_2 and another one at 532.2 eV from the remaining superficial oxides (CuO and ZrO_2, if present). It showed a reduction of Cu and Ce species in the catalyst after the reaction, being lower for the catalyst

Table 4 XPS data from SZXS and PROX materials

Sample	Si 2*p*	O 1*s*	S $2p_{3/2}$	Zr $3d_{5/2}$	Cu $2p_{3/2}$	I_{sat}/I_{pp}	% Ce^{3+}
SZ10S	103.0	532.0 (56%)	168.6	183.3	–	–	–
		532.9 (44%)					
SZ20S	103.4	532.0 (34%)	168.8	183.3	–	–	–
		533.1 (66%)					
SZ30S	103.3	532.0 (55%)	168.7	183.2	–	–	–
		533.0 (45%)					
SZ20Ce20Cu6	102.9	530.2 (44%)	–	182.3	934.2	0.48	14.0
		532.5 (56%)					
SZ20Ce20Cu6U	102.6	529.9 (39%)	–	182.0	932.8 (30%)	0.29	17.0
					934.8 (70%)		
SBACe20Cu6	102.7	529.9 (12%)	–	–	933.1 (29%)	0.45	17.5
		532.6 (88%)			935.4 (74%)		
SBACe20Cu6U	102.9	529.8 (12%)	–	–	932.5 (70%)	0.27	25.8
		532.4 (48%)			934.6 (30%)		

with SZ20 as support. It can be denoted with the change of Cu contributions and a decrease of the I_{sat}/I_{pp} ratio. It is a defined indicator of the amount of Cu^{2+} present in the surface of the sample, calculated by the ratio of satellite area (I_{sat}) and the principal peak (I_{pp}) of Cu $2p_{3/2}$ signal. These satellites "shake up" appear only when Cu^{2+} species are present. For bulk CuO the value of I_{sat}/I_{pp} is 0.55. Cu $2p_{3/2}$ core level signal can be decomposed in two contributions, according to previous works (Moretti et al. 2008; Reyes-Carmona et al. 2010). First one, at lower binding energy, assigned to partially reduced Cu species interacting strongly with ceria particles and another at high energy assigned to bulk CuO. Figure 9 presents a fully deconvoluted spectrum of Ce 3*d* and Cu 2*p* regions of SZ20Ce20Cu6 material.

3.2 Catalytic tests

Isopropanol conversion and 1-butene isomerization tests are widely used to obtain information about the catalytic properties of acid centers. Depending on whether the center is acidic or basic, the conversion of isopropanol will be carried to propylene or acetone, respectively.

3.2.1 Isopropanol dehydration test

These tests were performed under the operating conditions previously described. The same sample was used through the entire test, rising the temperature from 423 to 473 K, in steady state. Conversions obtained are presented in Fig. 10. While SBA-15 is not active in isopropanol conversion, the incorporation of ZrO_2 in this material generates acid sites, active in the dehydration of isopropanol to propylene. In the sample SZ10, the conversion increases with temperature and it is increased up to 43% at 473 K after sulfatation treatment. In the case of SZ20, the conversion of isopropanol reaches the 60% at 473 K. After impregnation with H_2SO_4, the conversion at low temperatures increases from 4% to 18% in SZ30S sample, but at higher temperatures, the conversion is lower than that of untreated samples. This decrease in conversion can be attributed to the substitution of Lewis acid sites with Brönsted type sites after the treatment and the formation of zirconium sulfate. The selectivity was technically reached 100% for propylene in all materials, detecting traces of di-isopropylether only at 473 K.

3.2.2 1-butene isomerization test

This test was also selected for evaluate the acidity of this family of materials, based on early works (La Ginestra et al. 1987; P. Patrono et al. 1994). The reaction is catalyzed by acid centers and occurs through a first step consisting of a double bond shifting, giving 2-butene (cis and trans), easily reaching the thermodynamic equilibrium. The isomerization to isobutenes in the second reaction step requires stronger acid sites. Measuring the ratio between cis and trans 2-butenes, the global conversion and the isobutene yield, we obtain an approximate distribution of acid sites of a catalyst. In our case, cis/trans ratio must be lower than 1, typical of acid catalysts (Suh et al. 2003).

In Fig. 11 the data obtained for the sulfated materials (SZXS) at 673 K are presented. In agreement with NH_3-TPD and isopropanol test data, SBA-15 is not active, while the incorporation of sulfated zirconia to the surface of SBA-15 allows high conversions, close to 70% for SZ10S sample. In all cases, cis/trans ratios are around 0.72, confirming the acid nature of these materials. The distribution of isomerization products is close in all cases due to the high space

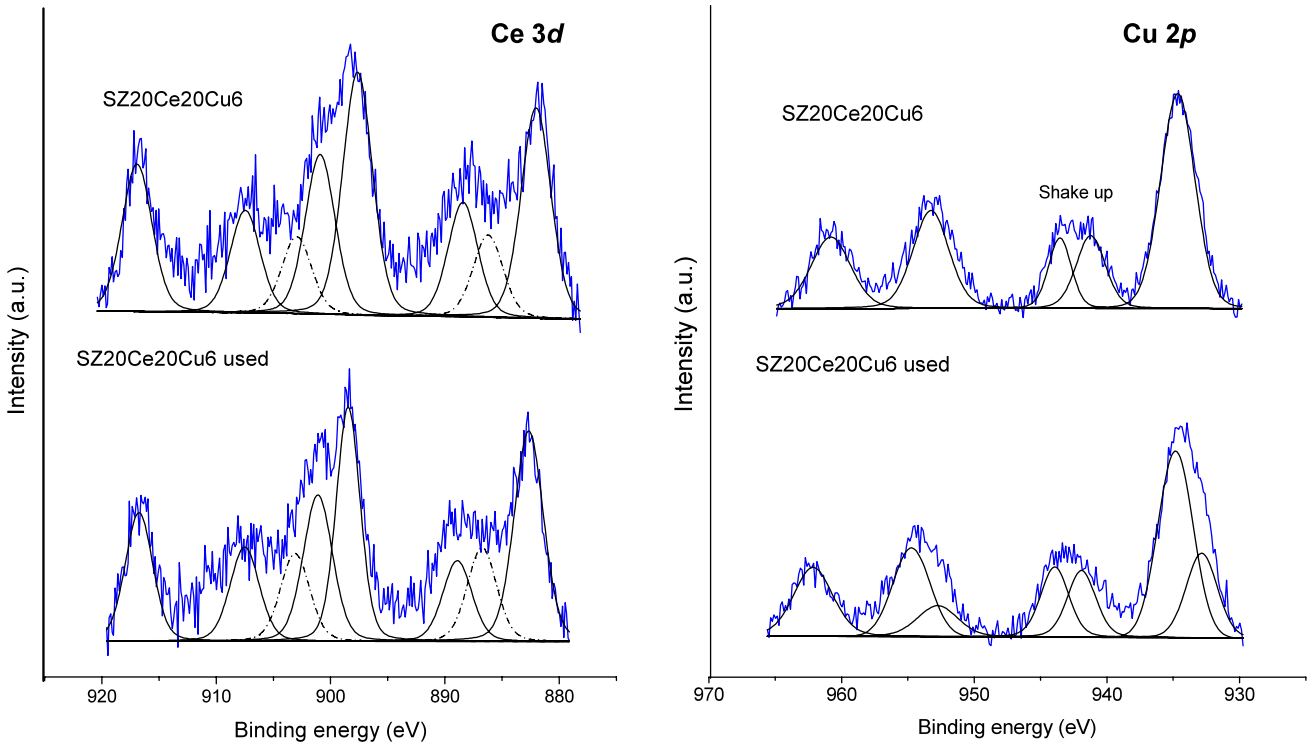

Fig. 9 Resolved X-ray photoelectronic spectra of Ce 3*d* and Cu 2*p* regions. *Dash-dotted* curves in Ce 3*d* spectra assigned to Ce^{3+}

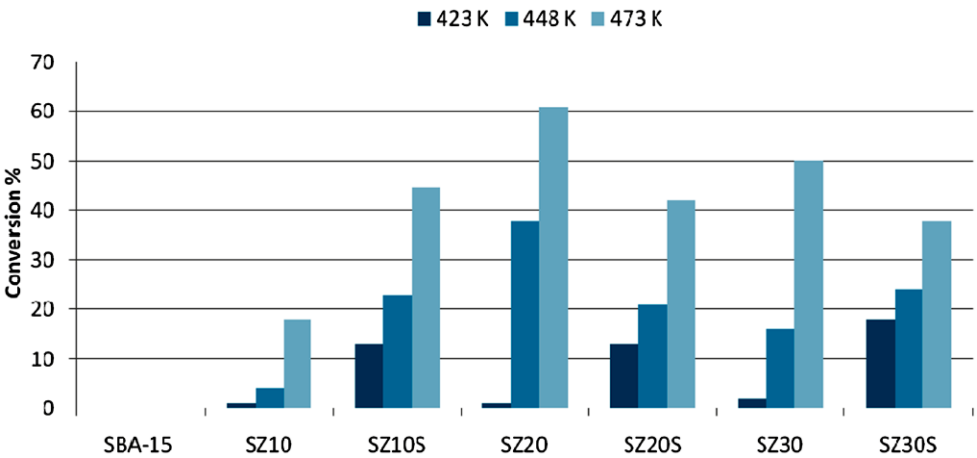

Fig. 10 Isopropanol conversion to propylene catalytic test for SZX and SZXS materials

velocity used to avoid the coke deposition over the sulfated samples.

3.2.3 CO-PROX reaction performance

Taking into account previous results, we found as optimal the SZ20 material, considering the active phase load, textural and acidic properties. The effect of the addition of Zr is not very clear, but seems to improve the dispersion and favor the reduction of copper oxide moieties on the material surface (Ratnasamy et al. 2004; Manzoli et al. 2005).

The synergic effect of Zr in CuO/CeO_2 catalyst was tested using pristine SBA-15 and SZ20 as supports with 20 wt.% of Ce and 6 wt.% of Cu. These Ce and Cu percentages were found optimal for CO-PROX reaction with an excess oxygen factor $\lambda = 2$ (Moretti et al. 2008, 2009). Both test results are shown in Fig. 12. Comparing both conversion-selectivity curves, a significant increment of conversion at low temperatures, in the 360–390 K range with a total selectivity to CO_2, is visible. At higher temperatures, 413–438 K, conversion reaches the 100% but a noticeable decrease of selectivity is observed, from 86 to 54%.The decrease of selectivity is thermodynamically fa-

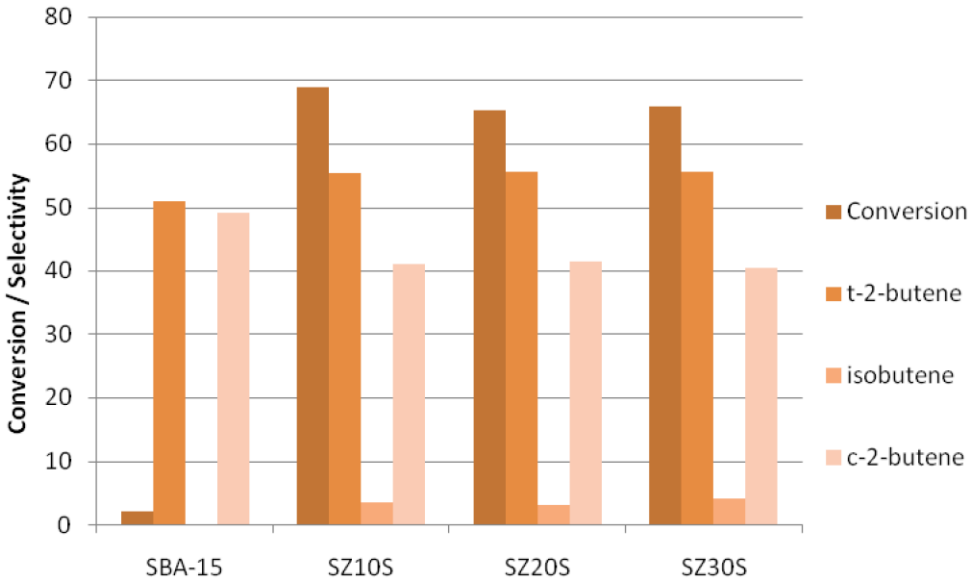

Fig. 11 1-butene isomerization test of SZXS materials at 673 K, after 2 hours of reaction

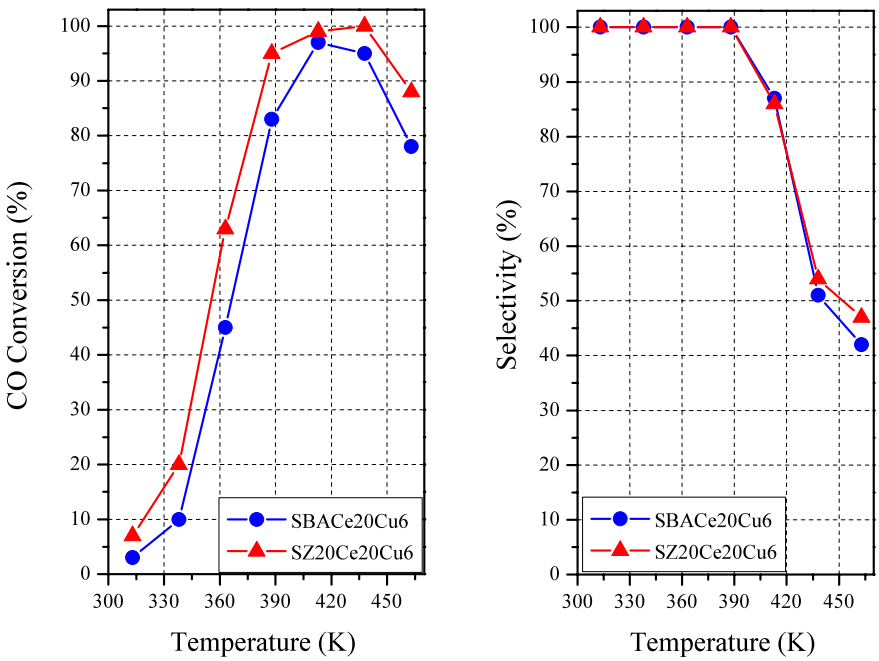

Fig. 12 CO-PROX reaction test using SZ20 and SBA-15 as supports with 20% Ce and 6% Cu (wt.). Operating conditions: 50% H_2, 1.25% CO, 1.25% O_2, He balanced, $\lambda = 2$, GHSV = 22000 h^{-1}

vored at higher temperatures by oxidation of hydrogen to water, which is the competitive reaction on PROX reaction.

4 Conclusions

A family of materials, based on mesoporous silica with zirconia incorporated, has been prepared. These solids exhibited high surface areas, with wide pores, good thermal resistance and acidic properties. The presence of high dispersed ZrO_2 nanoparticles was demonstrated by XRD and electronic microscopy techniques. These materials showed good acidic properties after treatment with sulfuric acid, which converts the zirconia particles in zirconium sulfate. Using several techniques, such as XRD, TPD-NH_3 and XPS, the presence of this sulfated zirconia was confirmed and then the samples were studied as good acidic materials with multiple potential catalytic applications. Their performance was tested in the isopropanol dehydration and 1-butene isomerization reactions. Finally, SZ20 sample was used as support of the redox couple system CuO/CeO_2 in the preferential oxidation of CO, showing a good catalytic performance in mild conditions, obtaining conversions of CO and selectivity to CO_2 close to 100%.

Acknowledgements The authors appreciate the financial support by projects MAT2009-10481, ENE2006-15116-C04-02 project (Ministry of Science and Innovation, Spain), FEDER funds, and the Junta de Andalucía through the Excellence Project P07-FQM-5070.

References

Akkari, R., Ghorbel, A., Essayem, N., Figueras, F.: Synthesis and characterization of mesoporous silica-supported nano-cristalline sulfated zirconia catalysts prepared by a sol-gel process: Effect of the S/Zr molar ratio. Appl. Catal. A **328**, 43–51 (2007)

Beck, J.S., Vartuli, J.C., Roth, W.J., Leonowicz, M.E., Kresge, C.T., Schmitt, K.D., Chu, C.T.W., Olson, D.H., Sheppard, E.W., Mccullen, S.B., Higgins, J.B., Schlenker, J.L.: A new family of mesoporous molecular sieves prepared with liquid crystal templates. J. Am. Chem. Soc. **114**, 10834–10843 (1992)

Berggen, A., Palmqvist, A.E.C., Holmberg, K.: Surfactant-templated mesostructured materials from inorganic silica. Soft Matter **1**, 219–226 (2005)

Corma, A., Juan-Rajadell, M.I., Lopez-Nieto, J.M., Martinez, C.: A comparative study of SO_4^{2-}/ZrO_2 and zeolite beta as catalysts for the isomerization of *n*-butane and the alkylation of isobutane with 2-butene. Appl. Catal. **111**, 175–189 (1994)

Fuxiang, L., Feng, Y., Yongli, L., Ruifeng, L.: Kechang, X.: Direct synthesis of Zr-SBA-15 mesoporous molecular sieves with high zirconium loading: characterization and catalytic performance after sulfated. Microporous Mesoporous Mater. **101**, 250–255 (2007)

Gómez-Cazalilla, M., Mérida-Robles, J.M., Gurbani, A., Rodríguez-Castellón, E., Jiménez-López, A.: Characterization and acidic properties of Al-SBA-15 materials prepared by post-synthesis alumination of a low-cost ordered mesoporous silica. J. Solid State Chem. **180**, 1130–1140 (2007)

Gracia, M.D., Balu, A.M., Campelo, J.M., Luque, R., Marinas, J.M., Romero, A.A.: Evidences of the in situ generation of highly active Lewis acid species on Zr-SBA-15. Appl. Catal. A, Gen. **371**, 85–91 (2009)

La Ginestra, A., Patrono, P., Berardelli, M.L., Galli, P., Ferragina, C., Massudi, M.A.: Catalytic activity of zirconium phosphate and some derived phases in the dehydration of alcohols and isomerization of butenes. J. Catal. **103**, 346–356 (1987)

Liu, W., Sarofim, A.F., Flytzani-Stephanopoulos, M.: Complete oxidation of carbon monoxide and methane over metal-promoted fluorite oxide catalysts. Chem. Eng. Sci. **49**, 4871–4888 (1995)

Liu, Y., Fu, Q., Stephanopoulos, M.F.: Preferential oxidation of CO in H_2 over CuO-CeO_2 catalysts. Catal. Today **241**, 93–95 (2004)

Manzoli, M., Di Monte, R., Boccuzzi, F., Coluccia, S., Kaspar, J.: CO oxidation over CuO_x-CeO_2-ZrO_2 catalysts: transient behavior and role of copper clusters in contact with ceria. Appl. Catal. B **61**, 192–205 (2005)

Martínez-Arias, A., Fernández-García, M., Gálvez, O., Coronado, J.M., Anderson, J.A., Conesa, J.C., Soria Munuera, G.: Comparative study on redox properties and catalytic behavior for CO oxidation of CuO/CeO_2 and CuO/$ZrCeO_4$ catalysts. J. Catal. **195**, 207–216 (2000)

Moretti, E., Lenarda, M., Storaro, L., Talon, A., Frattini, R., Polizzi, S., Rodríguez-Castellón, E., Jiménez-López, A.: Catalytic purification of hydrogen streams by PROX on Cu supported on an organized mesoporous ceria-modified alumina. Appl. Catal. B **72**, 149–156 (2007)

Moretti, E., Lenarda, M., Storaro, L., Talon, A., Montanari, T., Busca, G., Rodríguez-Castellón, E., Jiménez-López, A., Turco, M., Bagnasco, G., Frattini, R.: One-step synthesis of a structurally organized mesoporous CuO-CeO_2-Al_2O_3 system for the preferential CO oxidation. Appl. Catal. A **335**, 46–55 (2008)

Moretti, E., Storaro, L., Talon, A., Moreno-Tost, R., Rodríguez-Castellón, E., Jiménez-López, A., Lenarda, M.: CO preferential oxidation activity of CuO/CeO2 supported on zirconium doped MSU type silica. Catal. Lett. **129**, 323–330 (2009)

Park, D.E., Lee, D., Lee, H.C.: Recent progress in selective CO removal in a H_2-rich stream. Catal. Today **139**, 280–290 (2009)

Patrono, P., La Ginestra, A., Ramis, G., Busca, G.: Conversion of 1-butene over WO_3-TiO_2 catalysts. Appl. Catal. A **107**, 249–266 (1994)

Poulston, S., Parlett, P.M., Stone, P., Bowker, M.: Surface oxidation and reduction of CuO and Cu_2O studied using XPS and XAES. Surf. Interface Anal. **24**, 811–820 (1996)

Ratnasamy, P., Srinivas, D., Satyanarayana, C.V.V., Manikandan, P., Senthil Kumaran, R.S., Shetti Sachin, M., Vasudev, N.: Influence of the support on the preferential oxidation of CO in hydrogen-rich steam reformates over CuO-CeO_2-ZrO_2 system. J. Catal. **221**, 455–465 (2004)

Reyes-Carmona, Á., Arango-Díaz, A., Moretti, E., Talon, A., Storaro, L., Lenarda, M., Jiménez-López, A., Rodríguez-Castellón, E.: CuO/CeO_2 supported on Zr doped silica as catalyst for preferential oxidation of CO. J. Power Sources (2010). doi:10.1016/j.jpowsour.2010.10.019

Sohn, J.R., Seo, D.H.: Preparation of new solid superacid catalyst, zirconium sulfate supported on γ-alumina and activity for acid catalysis. Catal. Today **87**, 219–226 (2003)

Suh, Y.-W., Jung-Woo, J.-W., Lee, Rhee, H.-K.: Synthesis of thermally stable tetragonal zirconia with large surface area and its catalytic activity in the skeletal isomerization of 1-butene. Catal. Lett. **90**, 1–2 (2003)

Yadav, G.D., Nair, J.J.: Sulfated zirconia and its modified versions as promising catalysts for industrial processes. Microporous Mesoporous Mater. **33**, 1–48 (1999)

Zhao, D., Feng, J., Huo, Q., Melosh, N., Fredrickson, G.H., Chmelka, B.F., Stucky, G.D.: Triblock copolymer syntheses of mesoporous silica with periodic 50 to 300 angstrom pores. Science **279**, 548–552 (1998)